

ICJ



November 2016, Vol. 90, No. 11, Rs. 100. 68 pages.

THE INDIAN CONCRETE JOURNAL

PUBLISHED BY ACC LIMITED



Rigid Pavement

Probabilistic corrosion rates of cold-twisted deformed and thermo-mechanically treated steel in chloride-contaminated mortar

Jayachandran Karuppanasamy and Radhakrishna G. Pillai

The overall service life of concrete structures can be divided into corrosion initiation and corrosion propagation phases. Although the corrosion propagation period (t_p) is usually found to be smaller than the initiation period (t_i) it is important to estimate t_p for planning and budgeting for the repair activities. The t_p depends on the corrosion rate (i_{corr}) of the steel reinforcement. India has many old concrete structures built using the Cold Twisted Deformed (CTD) steel bars. Now-a-days, CTD steel (being highly vulnerable to corrosion) is rarely used and the Thermo-Mechanically Treated (TMT) or Quenched and Self-Tempered (QST) steel bars are extensively used. Quantitative information on i_{corr} of the CTD and TMT/QST bars are required for estimating t_p . However, very limited quantitative information is available on i_{corr} to estimate t_p . Therefore, the current practice is to assume that the i_{corr} of both CTD and TMT/QST steels are equal to that of plain mild steel, which might result in unrealistic estimations. This paper provides i_{corr} data obtained from 20-month long experimental program. The i_{corr} data were obtained using linear polarization resistance (LPR) tests on CTD and TMT/QST steel bars embedded in mortar. Twenty-five specimens were cast, cured, and subjected to a cyclic wet-dry exposure using 3.5 % sodium chloride solution. It is observed that the i_{corr} of CTD and TMT/QST steel bars can be represented as $\sim 3\text{PLN}(\sigma, \mu, \gamma)$; with $\sim 3\text{PLN}(0.3, 3.9, -24) \mu\text{A}/\text{cm}^2$ and $\sim 3\text{PLN}(0.2, 3.6, -20) \mu\text{A}/\text{cm}^2$, respectively. This corresponds to an average i_{corr} of 26.6 and 16.7 $\mu\text{A}/\text{cm}^2$, respectively, for CTD and TMT/QST steels. It is also found that, in general, i_{corr} of TMT/QST steel exhibits less scatter than CTD steel. This paper also provides the probabilistic estimations on t_p using the measured i_{corr} data and the t_p model developed by Wang and Zhao (1993). Based on the estimations, it can be concluded that the median time-to-crack for a system with CTD steel can be approximately 1.8 times less than that of a system with TMT/QST steel – indicating that early notification is required for engineers to prepare an optimized repair strategy for deteriorating structures.

Keywords: Corrosion rate; cold-twisted deformed; thermo-mechanically treated; quenched and self tempered; service life; corrosion propagation; probabilistic; time to crack.

1 INTRODUCTION

Service life of structures can be defined as the duration for which the structure is able to meet the desired performance with sufficient safety. Many structures are designed and constructed by keeping this in mind. However, many of the reinforced concrete structures show the signs of premature distress. The major reasons for this premature distress are overloading, aging of materials, aggressive environmental conditions, corrosion, inadequate maintenance, etc. The presence of oxygen, moisture, and chlorides can lead to the initiation of corrosion of reinforcement bars embedded inside

the concrete structure. Once initiated, it is almost impossible to stop corrosion. Due to prolonged corrosion, the cracking and spalling of the cover concrete can occur. This can further accelerate the corrosion process, which leads to a reduction in the structural capacity. In order to avoid unexpected/sudden failure and facilitate precautionary measures, the estimation of corrosion propagation period (t_p) and frequent performance monitoring of structure are essential. This paper focuses on determining the corrosion rate of two types of steel that are widely used in the concrete structures in India: (1) Cold-Twisted (CTD) and (2) Thermo-Mechanically Treated (TMT) [also known as Quenched and Self-Tempered (QST)]. Then, using the experimental data and a model

available in the literature, the probabilistic estimates of t_p for the reinforced concrete members with CTD and TMT/QST steels are estimated. The provided information can be used to strategize the repair and maintenance activities.

This paper is organized as follows. Next, review on the approaches for estimating service life is provided. Then, reviews of i_{corr} of various steel reinforcement and corrosion propagation models are provided. Following this, the significance of this research and the details on the experimental program are provided. Then, the experimental results and probabilistic estimations on t_p for the selected concrete systems with CTD and TMT/QST bars are provided.

1.1 Service life estimation

When a reinforced concrete structure is exposed to chloride environment, the chloride ingress towards the embedded steel reinforcement through the cover concrete. The deterioration process depends on many factors like the quality of concrete, available cover depth, concentration of chloride ions in the immediate environment, temperature and humidity conditions, diffusion coefficient of the concrete, and corrosion rate (i_{corr}) of the reinforcing steel bars (denoted as 'rebars', herein). Corrosion initiates when the concentration of chlorides deposited at the steel surface is more than the chloride threshold level. This instance is denoted as 'corrosion initiation point' as in Figure 1. Once corrosion is initiated, the rate of deterioration can be high due to the propagation of corrosion as indicated by the increase in the slope of the line in Figure 1. Most of the corrosion propagation models show that the t_p is comparatively very less than t_i . Thus, the time available to repair the corroding structural elements is very less once the corrosion is initiated.

To estimate the overall service life (i.e., $t_i + t_p$) of a structure, the data on (i) surface chloride content (C_s), (ii) chloride diffusion coefficient (D_{cl}), (iii) critical chloride threshold (Cl_{th}), (iv) corrosion rate (i_{corr}), etc. are the most influencing parameter considered. Because of multiple influential factors, the service life model should ideally be nonlinear in nature. Therefore, the bilinear assumption in Figure 1 may lead to an erroneous estimation for the structures. However, this is a reasonable assumption, especially for estimating t_p , and has been used by many researchers in the past.

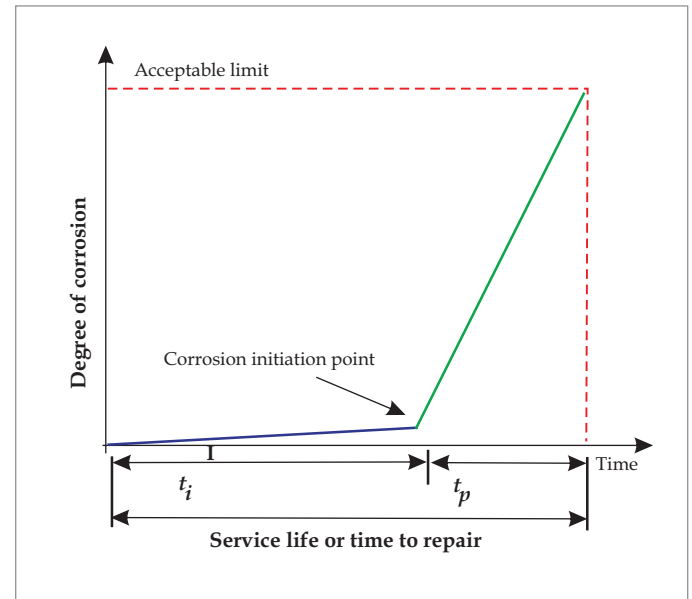


Figure 1. Service life of a reinforced concrete structure exposed to chlorides¹

Table 1. Wang and Zhao (1993) model to estimate the corrosion propagation period, t_p

Model to estimate t_p	Nomenclature
<p>Wang and Zhao (1993) [15]</p> $t_{cr} = \frac{H}{P_r}$ $\frac{\Delta}{H} = \gamma = 0.33 \left(\frac{D}{C_v} \right)^{0.565} f_{cu}^{1.436}$ $P_r = \left(\frac{W}{F \rho_{st}} \right) i_{corr}$	<p>t_{cr} is time required for cracking of cover concrete (years)</p> <p>W is the equivalent weight of steel (27.92 g)</p> <p>F is the Faraday's constant (96500 Coulombs)</p> <p>C_v is the thickness of concrete cover (mm)</p> <p>D is initial diameter of the bar (mm)</p> <p>f_{cu} is the cube strength of concrete (MPa)</p> <p>Δ is the thickness of corrosion product (mm)</p> <p>H is the depth of rebar penetration (mm)</p> <p>γ is the crack expansion coefficient of concrete</p> <p>ρ_{st} is the density of steel (7.85 gm/cm³)</p> <p>i_{corr} is the corrosion rate ($\mu A/cm^2$)</p> <p>P_r is the penetration rate (cm/s)</p>

A commonly used software program [2] to predict service life and estimate the life-cycle cost of concrete structures exposed to chloride environments, assumes a deterministic value of 6 years for t_p for systems with all types of steel reinforcement. This might not be appropriate, especially if the corrosion rates are different and probabilistic in nature. Thus, a probabilistic approach for estimating t_p is required for different types of steel used in reinforced concrete structures.

1.2 Corrosion propagation models

Researchers have attempted to model the cracking behaviour caused by corrosion using non-linear fracture mechanics and /or finite element analysis [3-15]. It might be too complicated to be used by practicing engineers. Researchers have also attempted to develop simple mathematical models to predict time to cracking (t_{cr}) - for easy use by practicing engineers. Each model requires different input parameters as per the corrosion mechanism and cracking process in concrete cover assumed.

Likewise, Wang and Zhao (1993) have developed a simple corrosion propagation model with linear assumption using corrosion rate [15]. This model assumes t_p as the t_{cr} after corrosion initiation. It is assumed that cracking of concrete will first occur when there is a certain quantity of corrosion

products forming on the reinforcement. This model considers the most commonly available parameters for the estimation of t_{cr} , which are provided in Table 1.

From the equations given in Table 1, it is evident that the empirical equation proposed by Wang and Zhao (1993) model, the compressive strength of concrete and i_{corr} of steel will be considered [15]. It is assumed that the corrosion product will fill the pores at the steel-cementitious interface and develop an expansive pressure on the cover concrete. The crack in cover will occur when the exerted tensile stress from the expansive corrosion product exceeds the tensile strength of the concrete. Thus, the Wang and Zhao (1993) model is preferred among many other empirical models. The time to cracking can be predicted from this model using the i_{corr} data measured from field and laboratory.

1.3 Corrosion rates of steel reinforcement

The i_{corr} is an important parameter required to estimate the corrosion propagation period (t_p), which is defined as the time between corrosion initiation time (t_i) and cracking of cover concrete (t_{cr}) [16]. The i_{corr} can be estimated using different techniques/measurements like linear polarization resistance (LPR), Electrical Impedance Spectroscopy (EIS), gravimetric mass loss. Table 2 shows the i_{corr} observed by many researchers for different steels embedded in chloride contaminated concrete systems.

Table 2. Corrosion rates of different steels embedded in chloride contaminated concrete systems

Steel type	Corrosion rate	Experimental details/environmental exposure conditions	Reference
Black steel	2.54 $\mu\text{m}/\text{yr}$	OPC concrete exposed to NaCl solution	18
	94 $\mu\text{m}/\text{yr}$	RC structure exposed to marine environment for 25 years	19
	16 to 32 $\mu\text{m}/\text{yr}$	Compared the available corrosion rates and developed equations	20
	0.025 to 1.620 $\mu\text{m}/\text{yr}$	OPC mortar exposed different NaCl concentration	21
	1 to 2 $\mu\text{m}/\text{yr}$	Embedded in different mortar with SCM, i_{corr} measured at corrosion initiation time	22
	0.026 to 1.575 $\mu\text{A}/\text{cm}^2$	OPC concrete with calcium nitrite exposed for 24 months	23
CTD	3 to 4.2 $\mu\text{A}/\text{cm}^2$	Embedded in different mortar with SCM, i_{corr} measured at corrosion initiation time	19
	77 to 111 $\mu\text{m}/\text{yr}$	Embedded in OPC mortar exposed for 3 months	24
TMT/QST	2.5 to 6 $\mu\text{A}/\text{cm}^2$	Embedded in different mortar with SCM, i_{corr} measured at corrosion initiation time	19
Galvanized steel	0.072 to 0.722 $\mu\text{A}/\text{cm}^2$	OPC concrete with calcium nitrite exposed for 24 months	23
Chromate treated galvanized steel	0.025 to 1.091 $\mu\text{A}/\text{cm}^2$	OPC concrete with calcium nitrite exposed for 24 months	23
Prestressing steel	3 to 9 $\mu\text{A}/\text{cm}^2$	OPC mortar; exposure period of 10 months	25

Table 3. Chemical composition of CTD and TMT/QST steel

Element	Cu	Co	Al	Ni	Mo	Cr	S	P	Mn	Si	C	Fe
CTD	0.09	0.01	0.01	0.07	0.01	0.07	0.27	0.09	0.45	0.23	0.13	remaining
TMT/QST	0.16	0.02	0.03	0.15	0.06	0.24	0.01	0.08	0.63	0.24	0.20	remaining

It should be noted that the performance of steel immersed in pore solution could not be well-correlated to that of mortar/concrete as the interface properties are very different [26]. Therefore, literature on the corrosion rates of TMT/QST bars obtained using (i) an external power source to drive the chlorides towards the steel and (ii) exposed to simulated pore solution are not included in this paper. It is observed that a few decades ago, gravimetric mass loss method was used by the researchers and represented corrosion rate in terms of mass loss ($\mu\text{m}/\text{year}$). Now-a-days, the trend is performing LPR technique and to represent i_{corr} in terms of corrosion current density (say, $\mu\text{A}/\text{cm}^2$).

The reason for such huge scatter in the i_{corr} can be due to the differences in the test methods, experimental setup, etc. Soylev et al. exposed bare black steel to 2, 3 and 4 % of sodium chloride solution and found the i_{corr} as 5.7, 6 and 10.7 $\mu\text{A}/\text{cm}^2$ respectively [16]. Pradhan et al. (2009) reported that the i_{corr} of CTD bars embedded in ordinary Portland cement (OPC) with various the water-cement ratios and different dosages of admixed chlorides ranges from 3 to 4.2 $\mu\text{A}/\text{cm}^2$ [2,17]. Pradhan et al. (2009) also reported i_{corr} for the TMT/QST steels with a range of 2.5 to 6 $\mu\text{A}/\text{cm}^2$. Thus, the i_{corr} may vary with different steel type, cementitious system, exposure conditions, and testing methods [17]. These variations in the reported i_{corr} values indicate that probabilistic estimations of propagation period, instead of deterministic estimations, are needed for service life estimation purposes.

2 RESEARCH SIGNIFICANCE

India has a significant number of concrete structures with CTD and TMT/QST steels. The corrosion rate (i_{corr}) is required to estimate the corrosion propagation period (t_p), which in turn is required for service life estimation. However, very limited information is available on i_{corr} for CTD and TMT/QST bars - making it difficult to estimate the service life. Current practice is to assume the same i_{corr} for plain mild steel, CTD, and TMT/QST steel, which may give

erroneous estimations of service life. In addition, software programs inadequately assume a constant value of 6 years for t_p , immaterial of the materials used. This paper provides experimental data and probabilistic distributions of i_{corr} of CTD and TMT/QST steel bars. Using these, the t_p values for various systems are estimated and compared using the models available in literature and other criteria. These findings can be very valuable to budget and plan repair strategies for the structures experiencing corrosion.

3 EXPERIMENTAL PROGRAM

3.1 Specimen design and preparation

An experimental program was conducted to obtain the long-term i_{corr} data for CTD and TMT/QST steel bars. Table 3 shows the chemical composition (determined using optical emission spectroscopy) of CTD and TMT/QST steels used. Twenty-five specimens (16 mm diameter and 420 mm long) were prepared and cleaned using the ASTM G1 (2011) [27]. To facilitate corrosion measurements, an insulated copper wire (300 mm long) was fastened to one end of the bar using a screw-thread system. Then, the steel bar (except the 50 mm length at the center) and the screw were coated with two thin layers of low viscosity epoxy.

Ordinary Portland cement (53 Grade) confirming the requirements of IS:12269-2008 was used [28]. Physical characteristics of cement were found as per IS:4031-200 [29]. The cement has the specific gravity of 3.16 and 30 % consistency. The fineness value was 310 m^2/kg as per ASTM C204 (2011) [30]. The initial and final setting time of the cement is 52 and 265 minutes, respectively. The oxide composition of the OPC cement was determined by X-Ray Fluorescence (XRF) spectroscopy and is presented in Table 4.

Silica sand (or Ennore sand) of Grades I, II and III, as classified in IS:383-1970 was used [31]. Distilled water was used for preparing all the cement mortar specimens.

Table 4. Chemical composition of ordinary portland cement (OPC)

Chemical component	Al_2O_3	CaO	Fe_2O_3	K_2O	MgO	Na_2O	SiO_2	SO_3
Concentration (%)	4.51	66.67	4.94	0.43	0.87	0.12	18.91	2.5

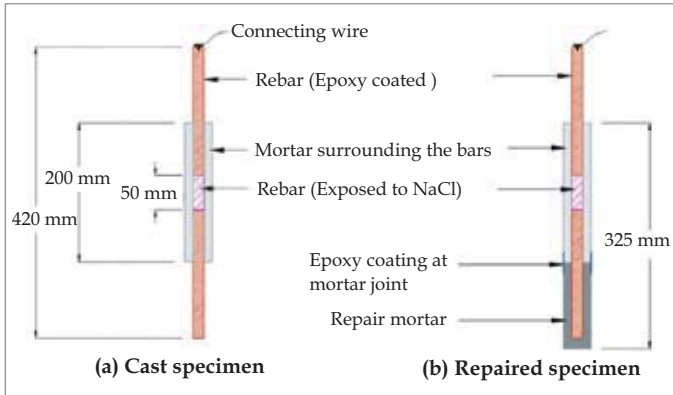


Figure 2. Test specimen with a steel bar embedded in mortar (a) and after repair (b)

Figure 2(a) shows a schematic diagram of the specimens prepared with the steel bars embedded in mortar with a water:cement:sand ratio of 0.55:1:2.75.

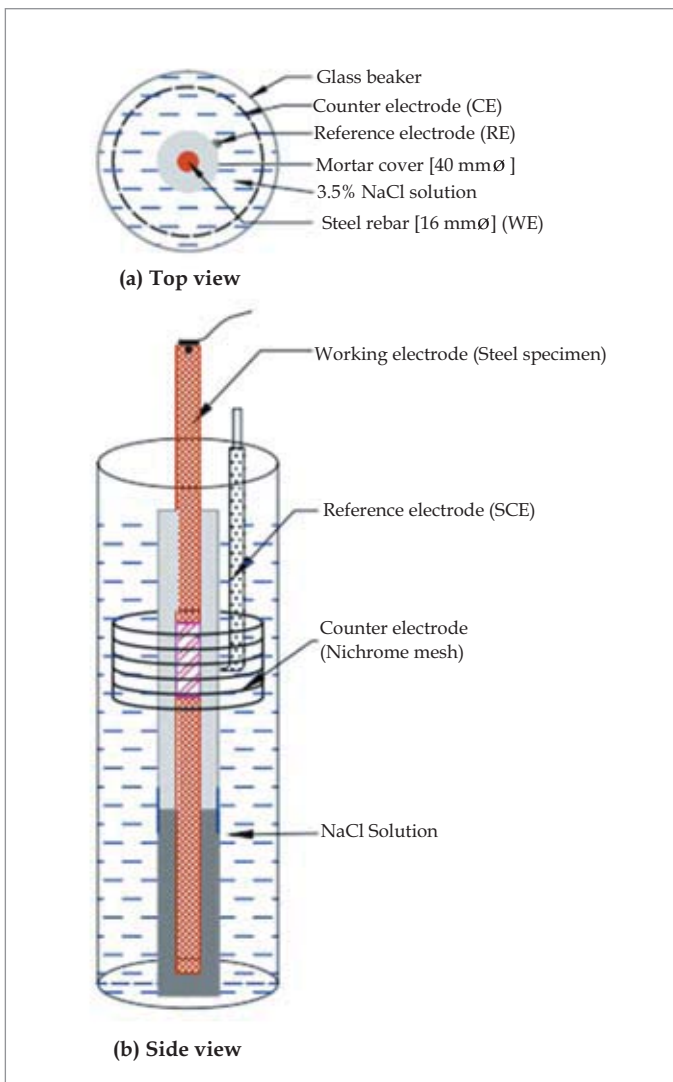


Figure 3. Schematic diagram of the 3-electrode corrosion cell setup [Top view and front view]

3.2 Curing and exposure conditions

The test specimens were cured in a laboratory environment (25°C and 65% RH approximately) for 24±1 hours. After this, the specimens were immersed/cured in saturated limewater for additional 27 days. The cured specimens were subjected to alternate wetting and drying cycle (i.e., 7 days wetting followed by 7 days drying) to accelerate the ingress of chlorides towards the embedded steel bar - thereby accelerating the corrosion initiation. 3.5 % sodium chloride (NaCl) solution was used for the wet-dry exposure, which was continued for a period of 20 months under laboratory environment.

3.3 Corrosion test setup

The Solartron 1287A potentiostat, a 3-electrode corrosion cell setup (see Figure 3) with a working electrode (WE), a counter electrode (CE), and a reference electrode (RE) were used to conduct the Linear Polarization Resistance (LPR) test. The central 50 mm uncoated region of the steel piece was considered as the WE. A 90 mm diameter pipe made of Nichrome wire mesh (24 wires per inch of 0.5 mm thick) was used as the CE. The test specimen was placed inside this CE. The saturated calomel electrode (SCE) was used as the RE and was placed at the surface of mortar cylinder (near the exposed steel portion at the center). All the electrodes were placed in a glass beaker with 3.5% NaCl solution. This corrosion cell setup was then connected to a potentiostat and computer for electrochemical measurements to conduct LPR test, as shown in Figure 4.

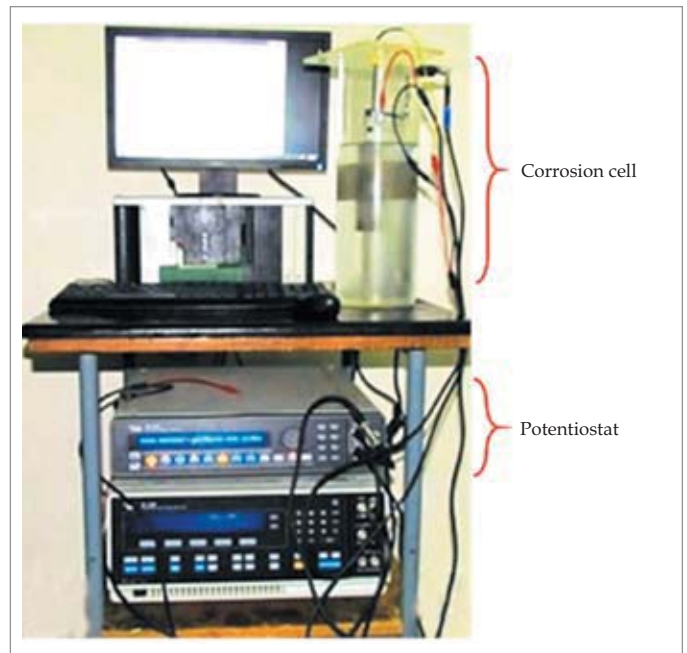


Figure 4. Corrosion test setup with corrosion cell, potentiostat (Solartron 1287), and computer

3.4 Corrosion measurement method

Corrosion measurements were taken at the end of the alternate wetting period (say, once in a month). At first, the Open Circuit Potential (OCP) of the steel specimen was measured. Immediately after measuring the OCP, the LPR test was conducted using a scan range of ± 15 mV with respect to the measured OCP of each specimen. A scan rate of 0.1667 mV/s was used. The measured current (I) was plotted with respect to the applied potential (E) to generate the LPR curve (see Figure 5).

The i_{corr} is calculated as given in the Eq. 1.

$$i_{corr} = \frac{B}{R_p} = \frac{B}{(\Delta E / \Delta i)_{E \rightarrow E_{corr}}} \text{ in } \mu\text{A}/\text{cm}^2 \quad \dots(1)$$

where, B is the Stern-Geary coefficient = 26 mV by considering active corrosion of the specimens, R_p is the polarization resistance ($\Omega \cdot \text{cm}^2$), ΔE is the applied potential (Volts), Δi is the measured corrosion current density (A/cm^2).

4 RESULTS AND DISCUSSION

4.1 Measured corrosion rate

As mentioned earlier, this paper focuses only on t_p , which mainly depends on i_{corr} of embedded steel rebar. Figure 6 and Figure 7 show the average of measured open circuit potential (OCP or E_{corr}) and i_{corr} of CTD and TMT/QST steels respectively, during the 20 months cyclic wet-dry exposure. After about two months of exposure, E_{corr} values are more negative than -276 mV vs SCE (equivalent to -350 mV versus

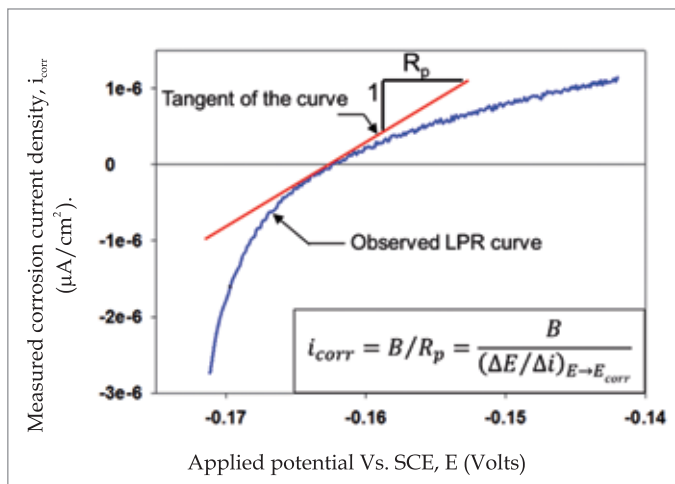


Figure 5. A typical linear polarization resistance (LPR) curve

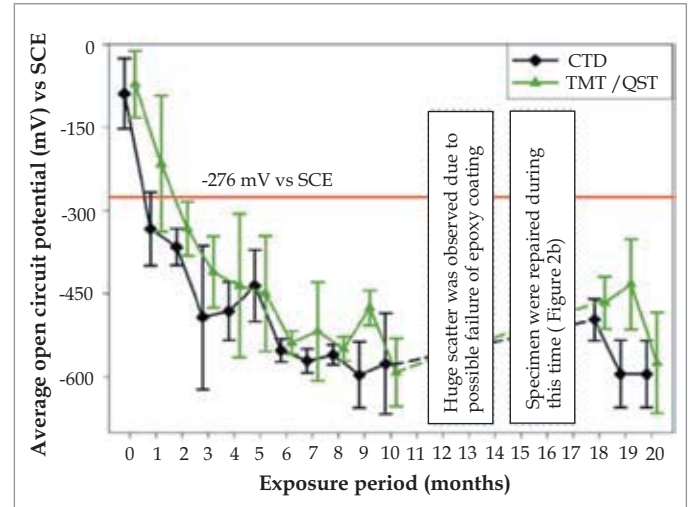


Figure 6. Average corrosion potential of CTD and TMT/QST bars

Cu/CuSO₄ electrode) - indicating that the specimens are experiencing 'active' corrosion.

The i_{corr} of both CTD and TMT/QST steels exhibit significant variations until about 5 months of exposure. Later, the i_{corr} exhibited similar reading or stabilized from about 5 to 10 months (with an approximate mean value of $15 \mu\text{A}/\text{cm}^2$ and COV 0.6). Unfortunately, the epoxy coating on the end portions of the steel specimens (a region with no mortar cover) failed/cracked after 10 months of exposure and led to severe under film corrosion (i.e., beneath the epoxy layer) and resulted in large i_{corr} , as shown in Figure 6.

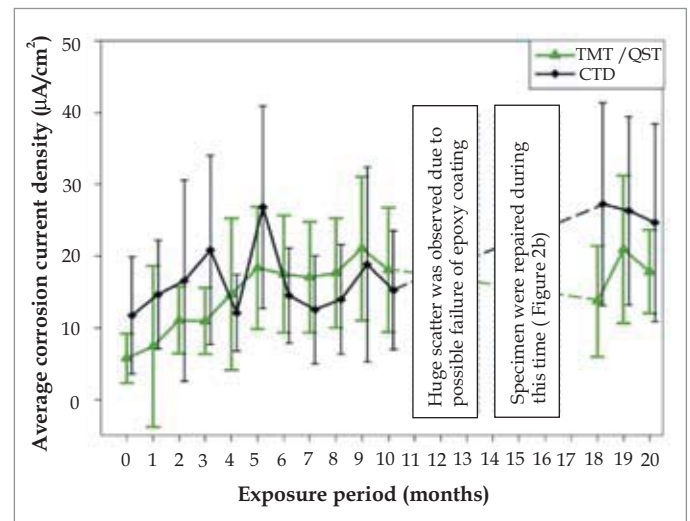


Figure 7. Average corrosion current density of CTD and TMT/QST bars

This data does not truly represent the i_{corr} of the predefined exposed surface at the centre of the specimen. Therefore, the epoxy coating and the under film corrosion products were removed, and the specimens were re-coated with 2 layers of epoxy. To avoid further failure/cracking of epoxy coating, the bottom part of the exposed steel was covered with cement mortar (denoted as 'repair mortar' in Figure 2b). After 28 days of curing, the repaired specimens were exposed to 3.5% NaCl solution and LPR testing was resumed at 18th month. The i_{corr} values measured from 18th to 20th month were used for estimating t_p and further analysis, shown later in this paper.

The results indicate that the tempered martensite surface layer of the TMT/QST bar exhibits higher corrosion rate at the beginning; then, decreased and became stable as a function of time. The CTD bars experienced higher corrosion rates than TMT/QST bars. This may be because CTD bars are strain hardened/cold-twisted during the manufacturing process. This process can lead to residual stresses and surface defects (at microstructure level) and when exposed to aggressive environments, CTD steel can experience stress-induced corrosion.

The i_{corr} data obtained for CTD bars exhibit huge scatter with a mean of $26.6 \mu A/cm^2$ and COV of 0.51. Likewise, the i_{corr} data obtained for TMT/QST bars exhibit a mean value of

$16.7 \mu A/cm^2$ and huge scatter with COV of 0.49. It should be noted that similar huge scatter has been observed in many literatures on corrosion rate in cementitious systems. For example, Paik et al. (1998) measured corrosion rates on reinforced concrete elements exposed to sea water and observed a COV ranges from 0.40 to 5 [32].

These have an underlying assumption that i_{corr} follows a normal distribution. However, i_{corr} must be a positive number and choosing a normal distribution for the i_{corr} is mathematically incorrect. This is because the data generated using a normal distribution might have negative numbers and can cause mathematical difficulties during simulation studies. [33] Also, Shapiro-Wilkinson normality tests were conducted for the i_{corr} data sets for both CTD and TMT/QST steels and it was concluded that the data sets do not follow a normal distribution. To find appropriate statistical distributions, histograms were generated using the data sets and suitable distributions were selected. The bin size of the histograms was chosen by the following conditions provided by the software [34].

- $n \leq 25$, then $b = 5$
- If $25 < n \leq 100$, then $b = n/5$
- If $n > 100$, then $b = 10 \times \log_{10}(n)$

where, n = number of data points and b = number of bins. Figure 9 shows the histograms with 10 and 25 bins for the same data. Both probability density function (PDF) curves with 3PLN and normal distributions seem to fit in the histogram with $b = 10$, but with $b = 25$, the 3PLN fits better than a normal distribution. Thus, the frequency of the data distributed over the entire data range is more important to select the suitable and common distribution form. To select a best-fit distribution based on the histogram, the value of b , determined using the software, is found inadequate for the

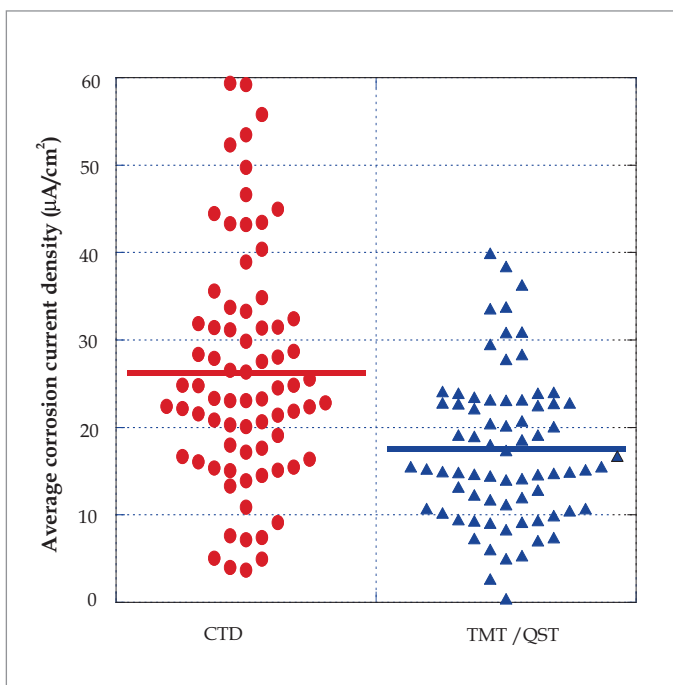


Figure 8. Measured corrosion rates

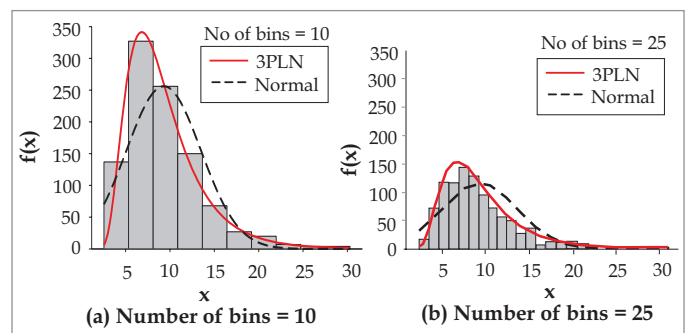


Figure 9. Histogram with different bin sizes

data obtained from 18 to 20 months of exposure Hence, the b value is assumed as 5 for all the cases in this study. This procedure is acceptable and followed by the commonly used statistical software packages [35,36].

With the obtained histograms, the data sets were compared with different distributions like Gaussian, Weibull, Gamma, Normal, Lognormal (LN), and 3-Parameter Lognormal (3PLN) and ranked for the goodness-of-fit with a confidence level of 90%, which has been used in corrosion studies including Saassouth et al. (2012 and Okeniyi et al. (2014) [37,38]. For the measured i_{corr} data for CTD and TMT/QST bars fits well with 3PLN distribution [LN (μ, σ, γ)]. It was found that a 3PLN distribution is suitable to represent the observed i_{corr} data. If i_{corr} is a random variable that has a 3PLN distribution, then $Y = \ln(X - \gamma)$ has a normal distribution with $N(\mu, \sigma)$. The probability density function of the 3PLN distribution, 3PLN(μ, σ, γ), can be calculated using the Eq. 2 [39].

$$f(x; \mu, \sigma, \gamma) = \frac{\exp\left\{-\frac{[\ln(i_{corr} - \gamma) - \mu]^2}{2\sigma^2}\right\}}{(i_{corr} - \gamma)\sigma\sqrt{2\pi}} \quad \dots(2)$$

where, μ is the scale parameter; σ is the shape parameter, γ is the location or threshold parameter. The limiting values of these parameters are: $-\infty < \mu < \infty, \sigma > 0$ and $X > \gamma \geq 0$, and The statistical mean and standard deviation of the random variable X , can be calculated by substituting the lognormal parameters in the Eq. 3 and Eq. 4 respectively.

$$Mean(i_{corr}) = \gamma + \exp\left(\mu + \frac{\sigma^2}{2}\right) \quad \dots(3)$$

$$SD(i_{corr}) = (\exp(2\mu + \sigma^2)(\exp(\sigma^2) - 1))^{0.5} \quad \dots(4)$$

where SD is the standard deviation. To confirm the obtained estimates, the same software program was used to obtain the parameter estimates as follows:

$$\begin{aligned} i_{corr} &\sim 3PLN(\mu, \sigma, \gamma) \\ &\sim 3PLN(0.26, 3.87, -23.66) \mu A/cm^2 \text{ for CTD bars and} \\ &\sim 3PLN(0.22, 3.6, -20.15) \mu A/cm^2 \text{ for TMT/QST} \\ &\text{bars for a period of 18}^{th} \text{ to 20}^{th} \text{ months} \quad \dots(5) \end{aligned}$$

Figure 10 (a) and (b) shows the histograms and the probability density functions of the representative lognormal distribution given in Eq. 5 for i_{corr} of CTD and TMT/QST bars respectively.

4.2 Probabilistic estimation of corrosion propagation periods

As mentioned earlier, Wang and Zhao (1993) considered the i_{corr} , cover depth (C_v), and compressive strength (f_{cu}) as the major influencing parameters, to estimate the corrosion propagation period (defined earlier as crack initiation period) [15]. In this analysis, a statistical distributions on i_{corr} , cover depth of 50 mm, and concrete compressive strength of 30 MPa are used. Figure 11 shows the probability density function (PDF) curves obtained for the CTD and TMT/QST steel bars, respectively.

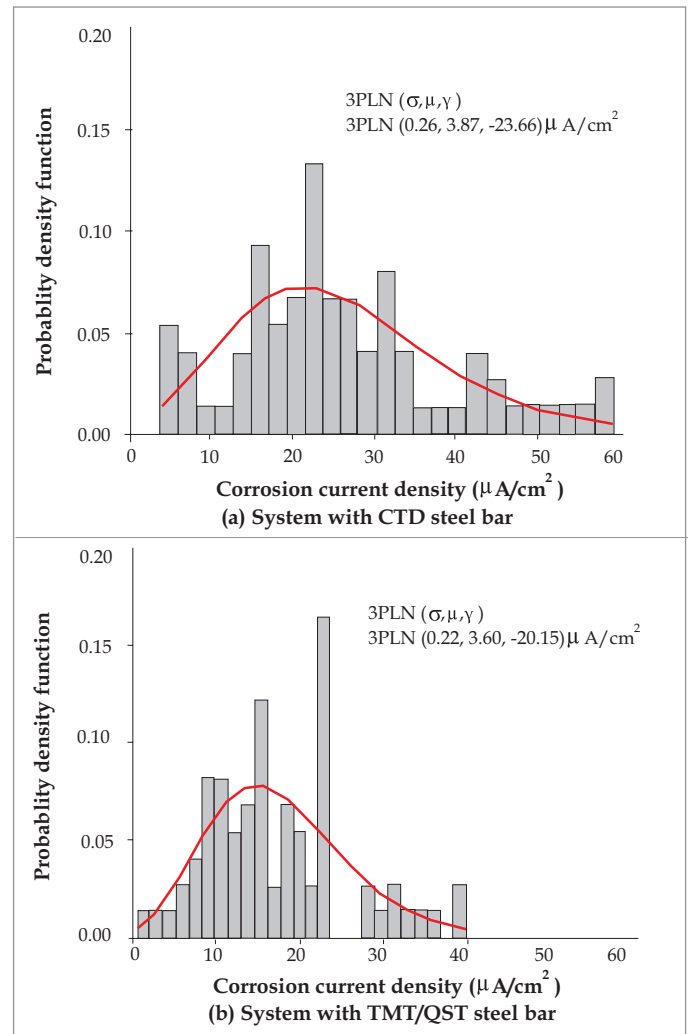


Figure 10. Histogram and PDF of i_{corr} for concrete systems with CTD and TMT/QST bars

Note that the PDFs are skewed (unlike normal distribution). For skewed distributions, median is a better statistic than mean and the vertical lines within the PDF curves indicate the median values, which are herein denoted as Median(t_p). The model by Wang and Zhao (1993) estimates that the $M(t_p)$ of 1.1 years with standard deviation of 1 year for CTD steel bars. Similarly, it estimates t_p of 1.75 years with standard deviation of 4.7 years for TMT/QST steel bars. The results indicate that the t_p for structures with TMT/QST steel bars is more than that for the structures with CTD bars. Based on experiments conducted under similar environmental exposure conditions and using same instruments/techniques, Karuppanasamy and Pillai reported that the mean value of i_{corr} for prestressing steels is $6 \mu A/cm^2$, which is, in general, less than the i_{corr} of both CTD and TMT/QST steels reported in this paper. [25] Another estimation by Andrade et al. indicates that the t_p can be between 2 and 10 years, if the i_{corr} of the steel is between 2.7 and $27 \mu A/cm^2$ [40]. Hence, a deterministic value for t_p for different steels may not provide a realistic estimation. However, the software program recommends a deterministic value of 6 years for t_p [2]. It should also be noted that the t_p estimated using Wang and Zhao (1993) model is less than the t_p of 6 years that is recommended by the software program is not conservative.

In RC structures, steel rebars are provided to take the tensile stresses. Typically, when the loss in the cross-sectional area of steel exceeds ~10% of the nominal cross-sectional area, a repair/rehabilitation/retrofitting work is recommended because of severe damage at that instant. Also, the concrete cover can crack before the loss in the cross-sectional area reaches 10%. Figure 11 shows that the t_p estimated for 10% area loss is 4.2 and 6.7 years for CTD and TMT/QST steel bars, respectively. Based on the estimated t_p , the concrete systems with CTD and TMT/QST steels may experience crack initiation in about 1.1 and 1.75 years, which is much less than the time-to-cracking (or corrosion propagation period, t_p , as defined earlier) of 6 years suggested by the software [2]. Therefore, it is recommended that the probabilistic distributions for i_{corr} presented in this paper and the Wang and Zhao (1993) model be used, instead of assuming 6 years, for assessing t_p for structures with CTD and TMT/QST steel rebars.

5 CONCLUSIONS

Based on the experimental program and the corrosion propagation models discussed in this paper, the following conclusions are drawn.

- When subjected to a cyclic wet-dry exposure to chloride environment, the corrosion rate, i_{corr} , of CTD

and TMT/QST steel bars can follow a 3-Parameter Lognormal distribution [3PLN (μ, σ, γ)] as follows:

1. CTD: $i_{corr} \sim 3PLN (0.3, 3.9, -24) \mu A/cm^2$
2. TMT/QST: $i_{corr} \sim 3PLN (0.2, 3.6, -20) \mu A/cm^2$

- For systems with 30 MPa concrete 50 mm cover depth and CTD steel bars and exposed to very severe chloride exposure conditions, the median of the time-to-cracking or corrosion propagation period (t_p) [i.e., Median(t_p)] is about 1 year after corrosion initiation. For similar case with TMT/QST rebars, this can be about 1.75 years.
- For systems with 30 MPa concrete, 50 mm cover depth and exposed to very severe chloride exposure

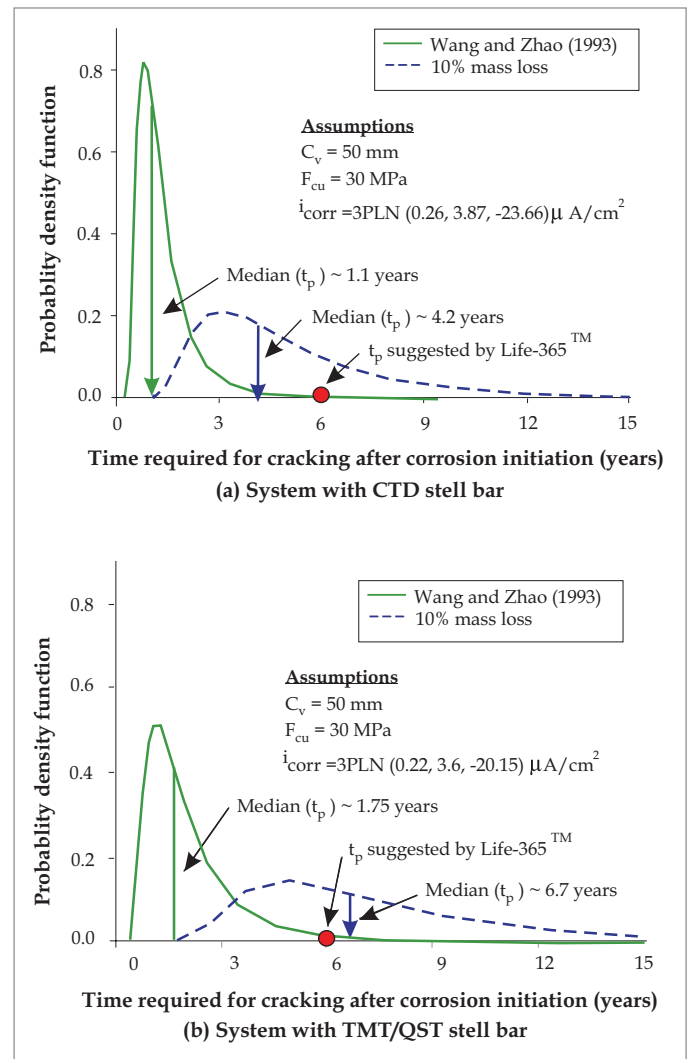


Figure 11. Estimated propagation period for concrete systems with CTD and TMT/QST bars

conditions, the Median(t_p) TMT/QST steel bars can be about 1.75 times more than that of a structure with CTD steel bars.

The present study can help the engineers to schedule and strategize suitable repair activities for the structures exposed to severe chloride conditions so that potential structural failures can be avoided.

Acknowledgements

The authors acknowledge the financial assistance from the Ministry of Human Resources Development (MHRD), Govt. of India and the Fast Track grant (Sanction No. SR/FTP/ETA-0119/2011) from Department of Science and Technology (DST), Govt. of India. The authors are thankful to Prof. Ravindra Gettu, Prof. Manu Santhanam, staff and students in the Building Technology and Construction Management Division, Department of Civil Engineering, IIT Madras for their priceless support and timely help.

References

1. Tutti K., Corrosion of Steel in Concrete, Report No. 4., Swedish Cement and Concrete Research Institute, Stockholm, Sweden, 1982.
2. Life-365™ v2.2.1, Life-365 Consortium III, Silica Fume Association, Lovettsville, www.life-365.org, 2014.
3. Cusson D., Lounis Z., and Daigle L., Improving performance prediction of corroding concrete bridges with field monitoring, Proceedings of the 6th International Conference on Concrete Under Severe Conditions Environment and Loading, June 7-9, 2010, Merida, Mexico.
4. Suwito C. and Xi Y., The effect of chloride-induced steel corrosion on service life of reinforced concrete structures, Structure and Infrastructure Engineering, 2008, Vol. 4(3), pp.177-192.
5. Chen D. and Mahadevan S., Chloride-induced reinforcement corrosion and concrete cracking simulation, Cement and Concrete Composites, 2008, vol.30(3), pp.227-238.
6. Liu, Y.; and Weyers, R., Modeling the time-to-corrosion cracking in chloride contaminated reinforced concrete structures. ACI Materials Journal, Vol. 95, Issue 6, pp. 675-681, 1998.
7. Molina, F. J., Alonso, C., and Andrade, C. Cover cracking as a function of rebar corrosion: Part 2 – Numerical model. Materials and Structures, 26(9), 532-548.
8. Bhargava, K., Ghosh, A. K., Mori, Y., and Ramanujam, S., Modeling of time to corrosion-induced cover cracking in reinforced concrete structures. Cement and Concrete Research, 35(11), 2203-2218., 2005.
9. Chernin, L., and Val, D. V., Prediction of corrosion-induced cover cracking in reinforced concrete structures. Construction and Building Materials, 25(4), 1854-1869, 2011.
10. Chernin, L., Val, D. V., and Volokh, K. Y., Analytical modelling of concrete cover cracking caused by corrosion of reinforcement. Materials and Structures, 43(4), 543-556, 2009.
11. Du, Y. G., Chan, A. H. C., and Clark, L. A., Finite element analysis of the effects of radial expansion of corroded reinforcement. Computers & Structures, 84(13-14), 917-929, 2006.
12. Jamali, A., Angst, U., Adey, B., and Elsener, B., Modeling of corrosion-induced concrete cover cracking: A critical analysis. Construction and Building Materials, 42, 225-237, 2013.
13. Jang, B. S., and Oh, B. H., Effects of non-uniform corrosion on the cracking and service life of reinforced concrete structures. Cement and Concrete Research, 40(9), 1441-1450., 2010.
14. Kim, K.H.; Jang, S.Y.; Jang, B.S.; and Oh, B.H., "Modeling mechanical behavior of reinforced concrete due to corrosion of steel bar", ACI Materials Journal, Vol. 107, Issue2, 106-113, 2010.
15. Wang X. M., and Zhao H.Y., The residual service life prediction of RC structures, In: Nagataki S., eds. Proceedings of the 6th international conference on Durability of building materials and components, Omiya, Japan. 1993. Ahmad S., Reinforcement corrosion in concrete structures, its monitoring and service life prediction – A review, Cement and Concrete Composites, 2003, Vol. 25, pp. 459-471.
16. Soylev T. A. and Richardson M. G., Corrosion Inhibitors for Steel in Concrete: State-of-the-art Report, Construction and Building Materials, 2008, Vol. 22, pp. 609-622.
17. Pradhan B. and Bhattacharjee B., Performance evaluation of rebar in chloride-contaminated concrete by corrosion rate, Construction and Building Materials, 2009, Vol. 23(6), pp.2346-2356.
18. Spellman D. L. and Stratfull R. F., Chlorides and Bridge Deck Deterioration, State of California Department of Public Works, Division of Highways, Materials and Research Department, Committee on Effect of Ice Control, 49th Annual Meeting, 1968.
19. Clear K. C., Measuring Rate of Corrosion of Steel in Field Concrete Structure, Transportation Research Record, No. 1211, 1992, pp. 28-38.
20. Hladky K., John D.G and Dawson J.L., Development in Rate of Corrosion Measurements for Reinforced Concrete Structures, Proceedings of the conference on Corrosion 89, 1989, NACE, Houston, TX, paper no. 169,
21. Ismail M. and Ohtsu M., Corrosion rate of ordinary and high-performance concrete subjected to chloride attack by AC impedance spectroscopy, Construction and Building Materials, 2006, vol. 20(7), pp. 458-469.
22. Hansson C. M., and Sorensen B., The Threshold Concentration of Chloride in Concrete for the Initiation of Reinforcement Corrosion, Corrosion Rates of Steel in Concrete, ASTM STP 1065, Berke N. S., Chaker V., and Whiting D., Eds, American Society for Testing and Materials, Philadelphia, 1990, pp. 3-16.
23. Berke N. S., Shen, D. F., and Sundberg K. M., Comparison of the Polarization Resistance Technique to the Macrocell Corrosion Technique, Corrosion Rates of Steel in Concrete, ASTM STP 1065, N S Berke, V Chaker, and D Whiting, Eds, American Society for Testing and Materials, Philadelphia, 1990, pp. 38-51.

24. Firodiya P., Sengupta A., and Pillai R. G., Evaluation of Corrosion Rates of Reinforcing Bars for Probabilistic Assessment of Existing Road Bridge Girders, *Journal of Performance of Constructed Facilities*, 2015, Vol. 29(3).
25. Karuppanasamy J., and Pillai R. G., Probabilistic Estimation of Corrosion Propagation Period for Prestressed Concrete Structures Exposed to Chlorides, *Proceedings of the 4th International Conference on Durability of Concrete Structures (ICDCS 2014)*, July 2014, Purdue University, West Lafayette, Indiana, USA.
26. Hansson, C. M., Poursaeed, A., and Laurent, A., Macrocell and microcell corrosion of steel in ordinary Portland cement and high performance concretes. *Cement and Concrete Research*, 2006, 36(11), 2098-2102.
27. Standard practice for preparing, cleaning, and evaluating corrosion test specimens, ASTM G1-2011, American Society of Testing and Materials, Conshohocken, PA, USA.
28. Specification for 53 grade ordinary Portland cement, IS:12269-2008, Bureau of Indian Standards (BIS), New Delhi, India.
29. Methods of physical tests for hydraulic cement, IS:4031-2008 (Part 1- 15), Bureau of Indian Standards (BIS), New Delhi, India.
30. Standard Test Methods for fineness of hydraulic Cement by air-permeability apparatus, ASTM C204-2011, American Society of Testing and Materials, Conshohocken, PA, USA.
31. Specification for coarse and fine aggregates from natural sources for concrete, IS:383-2002, Bureau of Indian Standards (BIS), New Delhi, India.
32. Paik, J., Kim, S., and Lee, S., Probabilistic corrosion rate estimation model for longitudinal strength members of bulk carriers. *Ocean Engineering*, 1998, 25(10), 837-860.
33. Hadley A. and Toumi, R., Assessing changes to the probability distribution of sulphur dioxide in the UK using a lognormal model, *Atmospheric Environment*, 2003, Vol. 37(11), pp.1461-1474.
34. @RISK, Palisade Corporation, West Drayton, Middlesex, UB7 7PN (UK), 2015.
35. EasyFit[®], MathWave Technologies, www.mathwave.com, 2014.
36. Sigmaplot[®], Systat Software Inc., 1735 Technology Drive Suite 430, San Jose, CA 95110, U.S.A. www.sigmaplot.com, 2015.
37. Saassouh, B., and Lounis, Z., Probabilistic modeling of chloride-induced corrosion in concrete structures using first- and second-order reliability methods, *Cement and Concrete Composites*, 2012, 34(9), 1082-1093.
38. Okeniyi, J., Ambrose, I., Okpala, S., Omoniyi, O., Oladele, I., Loto, C., and Popoola, P., Probability density fittings of corrosion test-data: Implications on $C_6H_{15}NO_3$ effectiveness on concrete steel-rebar corrosion, 2014, *Sadhana*, 39(3), 731-764.
39. Crow E.L., *Lognormal Distributions: Theory and Applications*, 1987, CRC Press, England.
40. Andrade C., Alonso C., and González J. A., Approach to the calculation of the residual service life in corroding concrete reinforcements based on corrosion intensity values, *Proceedings of the 9th European Congress on Corrosion 89*, 1989, Utrecht, Netherlands.



Jayachandran Karuppanasamy holds an M.E. degree in Construction Engineering and Management from College of Engineering, Guindy Campus, Anna University Chennai, India; Pursuing his PhD in the Department of Civil Engineering at the Indian Institute of Technology Madras, Chennai, India. His research interests include durability of building materials and corrosion mechanisms and service life estimation of concrete structures. He is also a Life Member of the Indian Concrete Institute (ICI).

Radhakrishna G. Pillai holds MS and PhD degrees in civil engineering from Texas A&M University, College Station, Texas, USA. He is an Assistant Professor in the Department of Civil Engineering at the Indian Institute of Technology, Madras, India. His research interests include corrosion control and testing, structures and materials performance, durability and service life estimation, repair and rehabilitation, grouting practices, and precast concrete construction. He is also a Life Member of the Indian Concrete Institute (ICI) and a senior member of RILEM.

